CT/有限要素法を用いた脊椎の圧縮強度解析
—骨粗鬆症治療効果判定への応用—

松本卓也

[共同演者]大西五三男，別所雅彦，大橋　暁，飛田健治，
中村耕三

東京大学医学部整形外科

1……目的，対象，方法

骨粗鬆症に対する薬剤効果判定として用いられるDXA法は，構造的強度評価は行えないため，精度と再現性を持つ定量的な骨強度予測法の開発が望まれる．先行研究として，新鮮椎体標本を単軸圧縮したものと，圧縮前にCT撮影して単軸圧縮力学試験と同様のシミュレーションモデルをつくったものを解析した結果，マイクロCTによる骨折線は，最小主ひずみの分布と近似しており，予測骨折荷重と実証実験の骨折荷重は高い相関があったことから，CT/有限要素法を骨粗鬆症の薬剤効果判定に応用した．

未治療の原発性骨粗鬆症女性17例を対象とし，リセドロネート(2.5 mg/日)群9例(平均62歳)，ラロキシフェン(60 mg/日)群8例(平均73歳)とした．投薬開始前と1年後にDXA，CT/有限要素解析，骨代謝マーカーを調べた．

2……結　果

骨代謝マーカーは，リセドロネート群では21%，ラロキシフェン群では27%で，それぞれ有意に減少した．1年後の骨密度増加率は，リセドロネート群ではDXAが平均3.7%，有限要素解析は平均6.9%で，ラロキシフェン群ではDXAが平均4.1%，有限要素解析は平均10.7%であった．

リセドロネート群でDXAが3.6%，解析値が11%増加した症例は，1年後に皮質骨シェル近傍と骨梁に沿った海綿骨の骨密度が増加し，最小主ひずみが減少して強度が上がっていた．また，ラロキシフェン群でDXAが8%，解析値が40%増加した症例も，1年後には皮質骨シェル近傍と，椎体内部の骨梁に沿って骨密度が増加し，最小主ひずみ分布が高い部分の面積が小さくなっていた(図1)．さらに，ラロキシフェン群でDXAが2.6%増加，解析値が18.2%減少した症例では，内部の縦の骨梁に沿って骨密度が増加しているようにみえたが，最小主ひずみの分布の高い部分が増加していた．CTの矢状断再構成では，形態的に皮質骨シェルの傾斜が前方に変化していたことから，形態変形が影響したと考えられる．

また，ラロキシフェン群でDXAが4.3%減少し，解析値が22%増加した症例は，骨密度が変化した場所が明確ではなかったものの，最小主ひずみ分布が減っていた中央前方寄りの部分では，骨梁が若干増えている印象があった(図2)．

まとめ

MORE試験では，3年間のラロキシフェン投与でDXAは数%の増加であったが，椎体骨折リスクは55%減少していた．また，治療前骨密度は骨折リスク判定に有用であるが，骨密度変化率での骨折リスク低下は証明できないことが報告さ

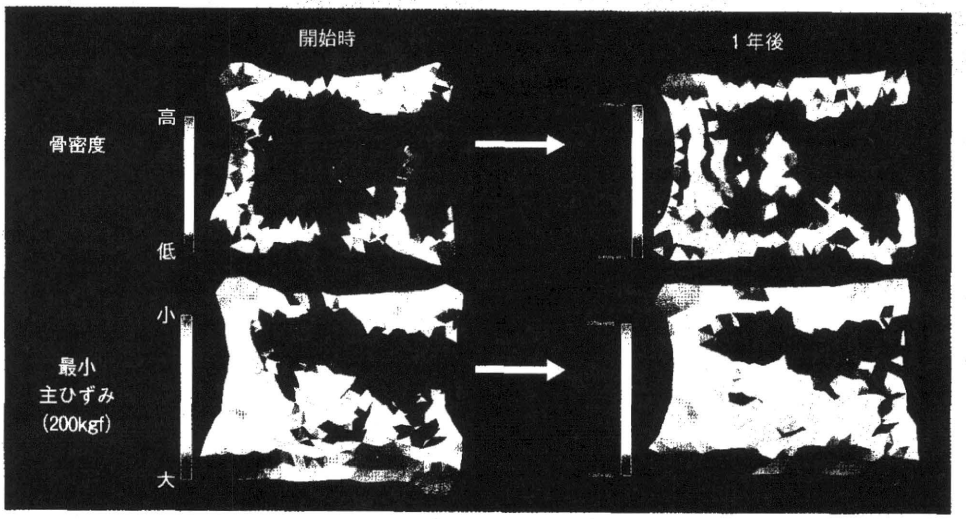

図1 症例1：ラロキシフェン
増加率：DXA 8.0%，解析値 40%.

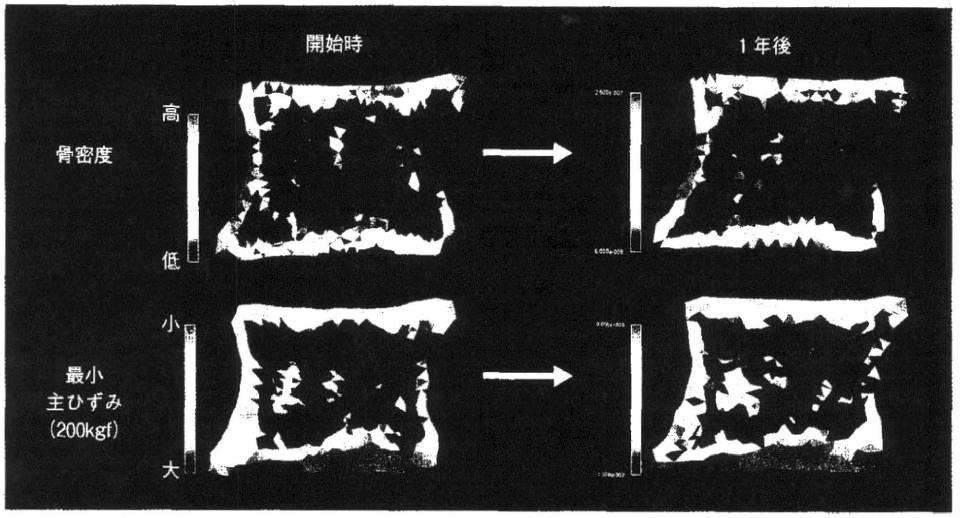

図2 症例2：ラロキシフェン
増加率：DXA −4.3%，解析値 22.2%.

れている.

本研究では，投薬による CT/ 有限要素解析の予測骨強度の変化は，骨密度の変化よりも高い傾向があり，この強度解析は，投薬による骨強度の変化を DXA 法よりも感受性高く検出できる可能性が示唆された．したがって，骨粗鬆症における薬剤効果判定に応用できる可能性があることから，さらに症例を増やして検討したいと考える.

大腿骨近位部の強度評価について
―CT/有限要素法による薬剤効果判定への応用について―

別所雅彦

[共同演者]大西五三男，松本卓也，大橋　暁，飛田健治，中村耕三

東京大学医学部整形外科

1……対象・方法

CT/有限要素法とは，定量的CT画像から3次元CTモデルを作成し，有限要素モデルに変換したものから実際のモデルを作成し，荷重拘束条件を設定して非線形解析により骨折荷重を予測する方法である．実際に大腿骨近位部標本を6回撮影して，再現性評価をすると変動係数(CV)％は1.1％であった．

骨粗鬆症に対する薬剤効果判定としておもに用いられるDXA法による評価は，骨折抑制率と必ずしも相関しないという報告もある．そこで，CT/有限要素法による予測骨強度評価法が，薬剤介入による骨強度増加を判定できるか検証するとともに，投与薬剤の違いによる治療効果判定を行った．

2……結　果

原発性骨粗鬆症未治療の女性15名を対象とし，リセドロネート(2.5 mg/日)群10名(平均62歳)，ラロキシフェン(60 mg/日)群5名(平均76歳)に投与し，服用開始時および1年後にDXA法による大腿骨頸部骨密度評価，定量的CTの撮影，および骨代謝マーカーを測定した．

1年後にリセドロネート群では，尿中デオキシピリジノリン(DPD)が服用開始時に比べ有意に21％減少し，ラロキシフェン群では，血清NTXが22％有意に減少した．

リセドロネート群では，予測骨折荷重は5.2％，頸部骨密度は2.0％といずれも有意に増加した．ラロキシフェン群でも予測骨折荷重は3.8％，頸部骨密度は2.9％と症例数の問題もあり，有意差はなかったものの増加傾向がみられた(図1)．

骨密度分布は，両群ともに1年後には主圧縮骨梁を中心に骨密度が増加しており(図2)，このために強度が増加したと考えられた．

実際にCT/有限要素法はCTから換算される骨密度であり，KeyakやKellerの理論に基づいて材料特性に変換している．ただ，薬剤効果判定する場合には，骨密度と材料特性の関係が崩れるという見方もある．

しかし，最近，ビーグル犬にリセドロネートを1年間投与した先行研究において，骨密度(体積分率)と降伏応力の関係に変化がないことが示されている．また，ビーグル犬にリセドロネートを1年間投与しても，骨密度とヤング率の関係に変化がなかったという報告もある．さらに，Keaveny らがアレンドロネート投与群とテリパラタイド群に関して，椎体で予測強度を比較したという発表もあり，徐々に薬剤効果にも，有限要素法が用いられる傾向にある．

まとめ

ラロキシフェンは，生理的な範囲内で骨代謝回

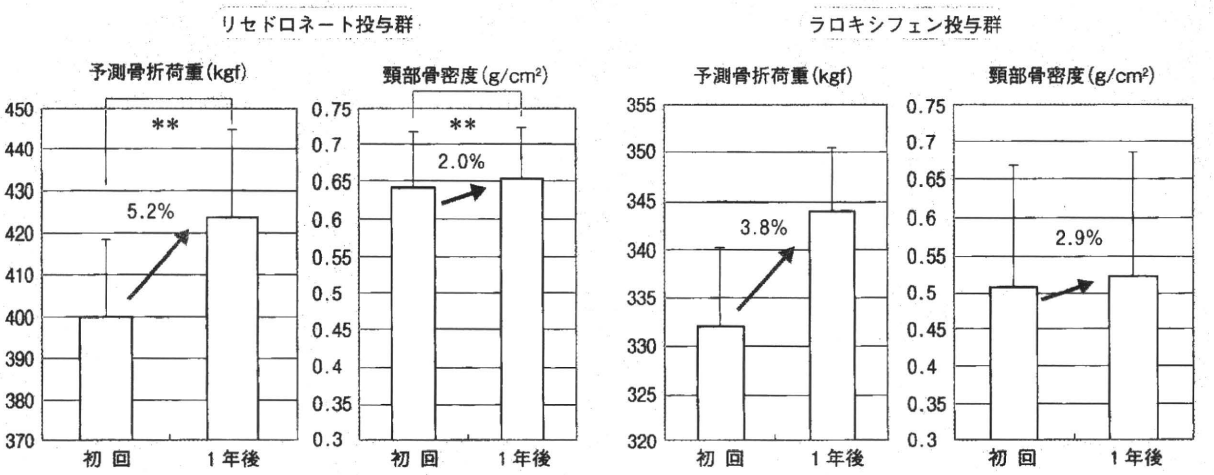

図1　CT/有限要素法(FEM)による予測骨折強度とDXA法による骨密度との比較

**：$P<0.01$

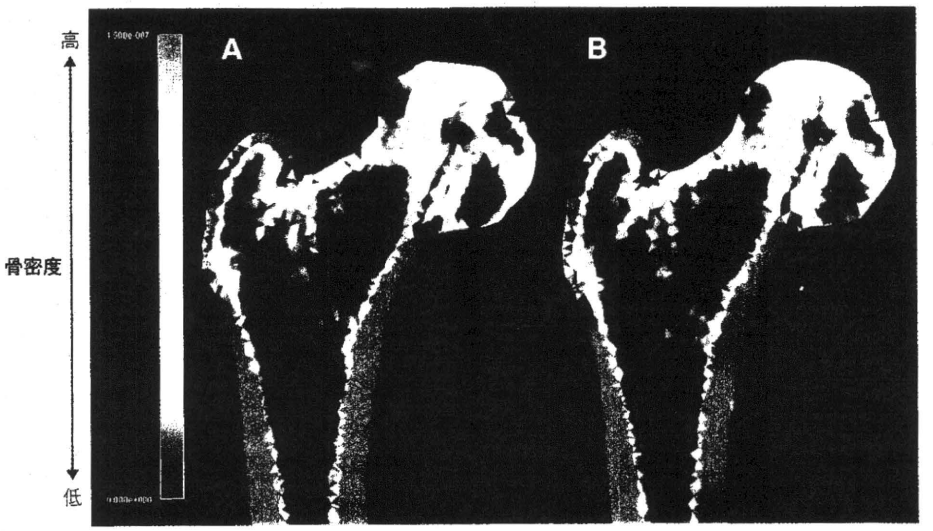

図2　ラロキシフェン投与群(79歳)

A：初回時(予測骨量荷重：330kgf，頸部骨密度0.168g/cm²)．B：1年後(予測骨量荷重：350kgf，頸部骨密度0.654g/cm²)．

転を改善すると言われていることから，ビスフォスフォネートで変化がないという結果が出ていれば，ラロキシフェンでも大きな変化はみられないと推測している．

以上より，薬剤効果による予測骨折荷重の増加は，検出可能であった．リセドロネート，ラロキシフェンともに，主圧縮骨梁を中心に骨密度が増加していた．DXA法による骨密度の変化より，CT/有限要素法の予測骨量の変化のほうが大きかった．

第10巻第3号／2008年10月31日発行　ISSN 1344-948

Vol.10 No.3 2008 Oct.

日本コンピュータ外科学会誌

Journal of Japan Society of Computer Aided Surge

第17回日本コンピュータ外科学会大会特集号

～安全と安心のための CAS ～

Special Number / 17th Annual Congress of Japan Society of Computer Aided Surgery

会　期：2008 年 10 月 31 日（金）・11 月 1 日（土）・2 日（日）
会　場：東京女子医科大学 弥生記念講堂　〒 162-8666 東京都新宿区河田町
大会長：伊関　洋　東京女子医科大学 先端生命医科学研究所

■ 特別企画
特別講演「医療再生」
特別シンポジウム「Women In Computer Aided Surgery」
パネルディスカッション(1)「医･理･工融合研究施設から発信する新しい医工
パネルディスカッション(2)
「レギュラトリーサイエンスからみた治療機器実用化のための問題点と解決

■ 一般演題
手術場・環境システム／セグメンテーション
VR・トレーニング・シミュレーション
内視鏡／手術機器・デバイス／ナビゲーション
画　像／ロボット・マニピュレータ
レギュラトリーサイエンス・安全評価／ポスターセッション

■ 教育セミナー要旨

協賛
ライフサポート学会，日本生体医工学会，日本ロボット学会，日本医用画像工学

08(XV)-71

CT/有限要素法を用いた新鮮死体大腿骨標本の予測骨折部位の検証

○ 別所 雅彦[a]、大西 五三男[a]、松本 卓也[a]、大橋 暁[a]
飛田 健治[a]、金子雅子[a]、中村 耕三[a]

[a]東京大学整形外科

Prediction of the fracture location of the proximal femur by a CT based finite element method

M. Bessho[a], I. Ohnishi[a], T. Matsumoto[a], M. Kaneko[a], S. Ohashi[a], K. Tobita[a], K. Nakamura[a]

[a] *The Department of Orthopaedic Surgery, The University of Tokyo, Tokyo, Japan*

Abstract: Hip fractures are the most serious complication of osteoporosis and have been recognized as a major public health problem. In elderly persons, hip fractures occur as a result of increased fragility of the proximal femur due to osteoporosis. It is essential to precisely quantify the strength of the proximal femur in order to estimate the fracture risk and plan preventive interventions. CT based finite element analysis could possibly achieve precise assessment of the strength of the proximal femur. The purpose of this study was to create a simulation model that could accurately predict the fracture location of the proximal femur using a CT based finite element method and to verify the accuracy of our model by load testing using fresh frozen cadaver specimens. Eleven right femora were collected. The axial CT scans of the proximal femora were obtained with a calibration phantom, from which the 3D finite element models were constructed. Non-linear finite element analyses were performed. A quasi-static compression test of each femur was conducted. FE analysis showed that the solid elements and shell elements in undergoing compressive failure were at the same subcapital region as the experimental fracture site..

Key words: Finite element method, Bone strength, Osteoporosis, Fracture site, Femur

1. 目的

骨粗鬆症が原因である大腿骨近位部骨折の患者は、近年、発生件数が年間約 12 万人となり、1987 年から比較すると、1992 年で 1.7 倍、2002 年で 2.2 倍となっており、年々確実に増えている[1]。現在の骨強度評価は、主に X 線写真および DXA(dual energy X-ray absorptiometry)による骨密度で評価されている。DXA 法による骨密度測定は、骨の立体的構造強度を定量評価できないという限界がある。こうした背景から、CT/有限要素法を用いて、骨強度を定量的に評価できる解析モデルの開発を行った。解析モデルの精確性の評価を行うために、新鮮凍結死体標本の圧縮試験を行った。前回[2]、骨折荷重の実験と解析の結果の相関が、r = 0.979 と高く、骨折荷重が正確に評価できることを報告した。今回、骨折部位に関して実験と解析の比較検討を行った。

2. 対象と方法

男性 5 人(30～90 歳　平均　56.8 歳)、女性 6 人(72～85 歳　平均　72.8 歳)から摘出した右大腿骨 11 本を使用した。倫理審査委員会の承認をへて遺族への説明同意を得た後に、死後 12 時間以内に採取し、実験まで凍結保存した。CT 画像、軟 X 線にて摘出大腿骨に骨折、ガン転移などの骨病変がないことを確認した。大腿骨は、小転子中央から遠位に 14 cm の部分で骨幹部を切断した。レジストレーション用にエポキシ樹脂マーカーを計 11 個、貼り付けた。CT (Aquilion Super 4、東芝メディカルシステムズ)を用いて、骨量ファントム (B-MAS200, 京都科学) とともに、検体を 3mm スライスで撮影を行った。圧縮試験は、大腿骨骨軸 20 度傾けて骨頭に対して準静的に圧縮を行った(Fig. 1)。実験後、骨折部位を確認するために 0.5mm スライスで CT 撮影を行った。一方、定量的 CT から、海綿骨に 3mm の 4 節点ソリッド要素と、皮質骨外層に 0.4 mm の 3 節点シェル要素を使用し、3 次元骨強度解析モデルを作成した。骨は不均質材料とし、重量密度は各要素に対して骨量ファントムの CT 値から換算式により計算した。材料特性は各要素の位置に対応する重量密度から個々に算出し、これに対応する要素の材料特性に割り当てた。

ヤング率はKeyak [3]ら、およびKeller [4]らの方法により設定した。ポアソン比は、0.4とした。荷重条件および拘束条件は、骨軸から20度内側に傾けた方向で骨頭を圧縮し、骨幹部遠位端を拘束した条件とした。

Newton-Raphson 法を用いた荷重増分法による非線形解析を行い、1つのシェル要素の最大主応力がその要素の臨界応力を超える場合（クラック）、または、1つのシェル要素のDrucker-Prager 相当応力が要素の降伏応力を超え、かつ最小主歪みが-10000 micro strain以下の場合(圧潰)をそれぞれ骨折と定義した。1要素以上の破壊を骨折と定義し、予測骨折荷重を解析した。

実験での骨折部位と予測骨折部位を比較対照した。また、骨折部位と解析での最小主ひずみ分布の比較も行った。

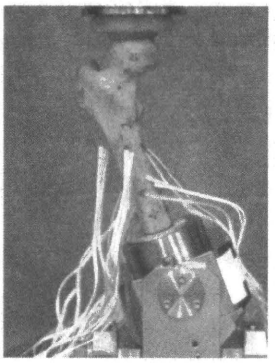

Fig. 1: Uniaxial compressive loading testing

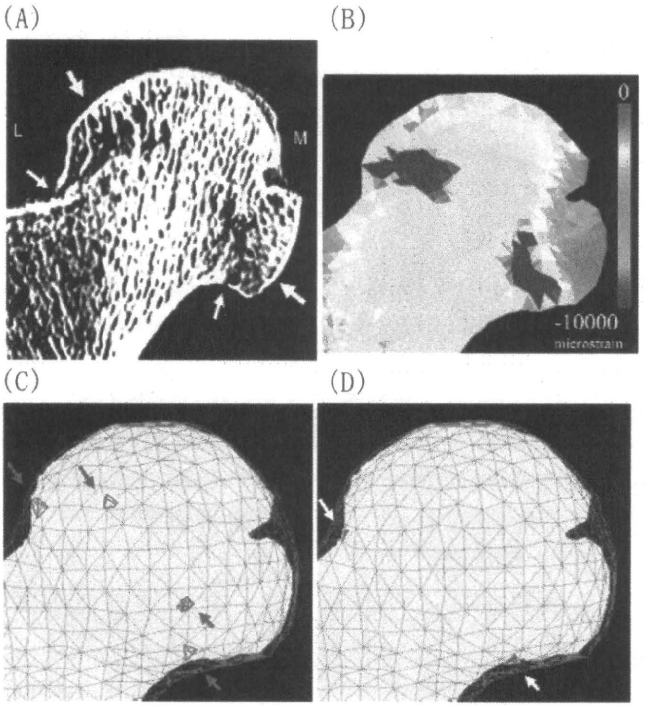

Fig. 2: (A) Fracture sites in a tested specimen (FR02). The arrows indicate the fracture site. The specimen sustained a fracture of the subcapital region. (B-D) Predicted fracture sites. (B) The minimum principal strain distribution under the predicted fracture load is shown for a mid-sagittal section by the FE model. The area with the lowest minimum principal strain is at the subcapital region. (L; lateral, M; Medial). (C) The failed tetrahedral elements in the mid-sagittal section (arrows) predicted by FE analysis. (D) The failed triangular elements in the mid-sagittal section (arrows) predicted by FE analysis.

3. 結果

11検体すべてにおいて大腿骨頭下に骨折が発生していた。また、実験での骨折部位は、予測骨折部位とほぼ一致していた。また、最小主ひずみ分布は骨折分布とほぼ一致していた (Fig. 2)。

4. 考察

先行研究では、Keyak ら[5]が実際の骨折部位と予測骨折部位比較しているが、骨折部位をCT等で正確に検証していない。我々の CT/有限要素法モデルは、骨折荷重ばかりではなく骨折部位も予測可能であることが検証された。

文献

1) Yoshimura, N., Suzuki, T., Hosoi, T. and Orimo, H., Epidemiology of hip fracture in Japan: incidence and risk factors. Journal of Bone and Mineral Metabolism 2005;23 Suppl:78-80.
2) 新鮮死体大腿骨標本のCT/有限要素法による予測骨折荷重の正確性の検証，別所雅彦，大西五三男ら、日本コンピュータ外科学会誌、2007、9巻3号 Page 274-275
3) Keyak, J. H., Lee, I. Y. and Skinner, H. B., Correlations between orthogonal mechanical properties and density of trabecular bone: use of different densitometric measures. J Biomed Mater Res 1994;28:1329-36.
4) Keller, T. S., Predicting the compressive mechanical behavior of bone. J Biomech 1994;27:1159-68.
5) Keyak, J.H., et al., Prediction of fracture location in the proximal femur using finite element models. Med Eng Phys, 2001. 23(9): p. 657-64.

直達式骨折整復を支援する骨折整復システムの開発

鄭常賢[1], 加門大和[1], 廖洪恩[2], 光石衛[2], 中島義和[2],
小山毅[4], 菅野伸彦[4], 前田ゆき[5], 別所雅彦[3], 大橋暁[3], 松本卓也[3],
岩城純一郎[6], 中沢東治[6], 大西五三男[3], 中村耕三[3], 佐久間一郎[2]
東京大学大学院 {[1]新領域創成科学研究科, [2]工学系研究科, [3]医学系研究科},
[4]大阪大学大学院医学系研究科, [5]大阪南医療センター, [6]THK(株)

骨粗鬆症がある患者におこりやすい骨折のなかでも大腿骨頚部骨折は寝たきりとなる可能性の高い骨折である．社会の高齢化の進行に伴い骨粗鬆症の患者が増加すると，大腿骨頚部骨折の患者も増加すると予測されている．

大腿骨頚部骨折の治療法は外科的な手術によるものがほとんどである．手術では大腿骨の遠位骨片を牽引しながら位置決めし，ピンによって固定する．しかし，大腿筋などの周辺組織が萎縮した状態では整復のための牽引に大きな力が必要となるため術者にとって負担となる．また，X 線透視下で 2 次元の情報を用いて位置決めを行わなければならないため，術者の熟練が必要であり，手術を行うことで術者が受ける X 線被爆も問題である．

これらの問題に対し，我々は骨折整復システムの開発を行った（Fig. 1）．システムは骨折整復ロボットとナビゲーションシステムに構成されている．骨折整復には，足首をつかみ遠位骨片の位置を合わせる介達式骨折整復方法と，骨片にピンを打ち，ピンに連結されたリングを持って直接整復を行う直達式骨折整復方法がある．骨折整復システムは介達式骨折整復に対して使えるように構成されているが，ロボットを使う利点を考えると骨片の正確な位置決めが可能な直達式骨折整復にも使用されるように構成する必要があり，今回は新たに直達式骨折整復を直達式骨折整復ロボットに実装を行った．

骨折整復ロボットは並進 3 自由度と回転 3 自由度の 6 自由度を有する．骨片の牽引と回旋をするときの整復力が設定値より大きくなると各関連軸をフリーにするフェイルセイフ装置が装着されており安全性を保つ．動作モードはタッチパネルを用いたジョグモード，術者の整復力をパワーアシストする手動モード，ナビゲーションからの指令により自動で整復を行う自動整復モードがある．

直達式整復では，骨とロボットの手先は専用のジグで繋がっているので，骨の長軸とロボットの牽引軸が一致しない．骨片の姿勢だけを変えるため，骨折断面の中心を仮想中心と見なし，ロボットを制御する拘束パワーアシストを実装し，有効性を検証した．

ナビゲーションシステムは術前に CT からの 3 次元モデルを用いて整復ゴールを計算する．術中には C-arm で撮った画像と 3 次元モデルをレジストレーションすることにより，実空間での骨片間の位置関係を認知する．骨片の現在位置からゴールまでの整復パスは術者の意見を反映して作成され，整復ロボットに指令を送り整復を行う．構成したシステムは骨折モデルでの整復実験でその有効性を示す．

Fig.1.骨折整復システム

直達式骨折整復支援装置を用いた整復動作に関する研究
Study on Fracture Reduction Assistance Computerized Robot

○加門 大和[1], 鄭 常賢[2], 廖 洪恩[2], 小林 英津子[1], 光石 衛[1], 中島 義和[1], 小山 毅[4], 菅野 伸彦[4], 前田 ゆき[5], 別所 雅彦[3], 大橋 暁[3], 岩城 純一郎[6], 中沢 東治[6], 大西 五三男[3], 佐久間 一郎[1]
東京大学大学院{1. 工学系研究科, 2. 新領域創成科学研究科, 3. 医学系研究科},
4. 大阪大学大学院医学系研究科, 5. 大阪南医療センター, 6. THK
○H.Kamon[1], S.Jhoung[2], H.Liao[2], E.Kobayashi[1], M.Mitsuishi[1], Y.Nakajima[1], T.Koyama[4], N.Sugano[4], Y.Maeda[5], M.Bessho[3], S.Ohashi[3], J.Iwaki[6], T.Nakazawa[6], I.Ohnishi[3], I.Sakuma[1]
{1. Graduate School of Engineering, 2. Graduate School of Frontier Sciences,
3. Graduate School of Medicine}, the University of Tokyo ,
4. Graduate School of Medicine, Osaka University,
5. National Organization Osaka Minami Medical Center, 6. THK

1. はじめに

大腿骨頚部骨折は高齢者に起こりやすい骨折で，社会の高齢化の進行に伴って患者も増加すると予想される．手術では遠位骨片を牽引・回旋しながら位置決めし，骨折部位をピンなどで固定する．しかし大腿骨の周辺の筋は牽引を妨げるので，大きな力が要る．また，骨折部位の仮骨形成を早めるためには，骨片間距離を2[mm]，2[degrees]以内に収める必要がある．[1]しかも，X線透視下で2次元画像による位置決めを行うため，熟練した技術が必要である．術者が受けるX線も問題である．

この問題に対し，我々はロボットで牽引を補助し，医師の負担を減らす．このロボットに，骨軸に沿うようにロボットの駆動方向を拘束するという，拘束パワーアシスト(Fixed Power Assistance: FPA)の実装した骨折整復支援装置(Fig. 1)の開発を行っている．本研究では，直達牽引骨折整復支援装置を用いた拘束パワーアシストによる骨折整復動作の動作精度を評価した．

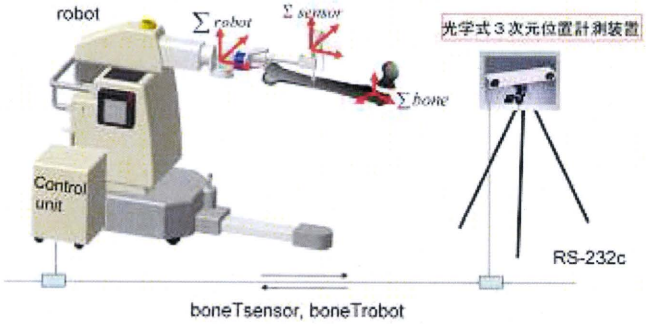

Fig. 1 骨折整復支援装置(ロボット)とシステム構成

2. システム構成

システムの流れを Fig.2 に示す．光学式三次元位置計測装置を使用してロボット座標・力センサ座標・骨座標の位置を計測し，力センサと骨，ロボットと骨の対応関係を算出する．力センサに入力した力情報(術者の力)を骨座標での力情報に変換し，骨片を移動させない方向(例えば骨軸に沿わない牽引・回旋方向等)の力成分をゼロに設定する．その結果得られた力ベクトル方向に骨片が移動するように目標位置を定め，その位置へ駆動するためのロボットの逆運動学計算を行い，速度指令を生成する．

3. 実験および結果

骨片の位置決めは牽引動作と回旋動作の2つに分けて行われているので，それぞれの動作について精度評価を行った．計測には光学式三次元位置計測装置を用いた．

牽引動作は骨の長軸方向に牽引した．骨の長軸ベクトルと計測点から得られる近似直線ベクトルがなす角を評価した．要求仕様が 2[degrees]に対して 0.25[degrees]という高精度で牽引できた．

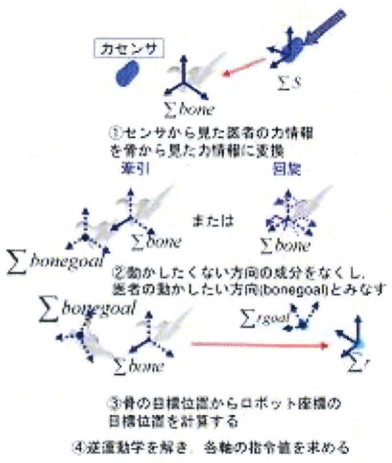

Fig. 2 FPA の駆動方式

回旋動作は骨が 0.2[deg/s]で回旋するように各軸モータに指令した．骨座標の各軸周りにそれぞれ回旋し，骨の位置の変化量を評価した．要求仕様が 2[mm]であるのに対し，平均誤差は 5.9[mm]と大きな値となった．これは，ロボットに機構的なガタがあることが原因と考えられる．

4. まとめ

FPA の精度評価を行い，牽引動作については目的とする精度での拘束が可能であったが，回旋動作については装置のガタや指令速度遅れ等が原因となり，必要となる拘束精度を実現することはできなかった．今後は装置のガタを修理して回旋動作の精度を高くし，モデル脚で FPA の有効性を評価する予定である．

5. 謝辞

本研究の一部は厚生労働科学研究費補助金(医療機器開発推進研究事業)「低侵襲・高精度骨折整復・治療支援システムの開発(H20-ナノ-一般-002)」，厚生労働科学研究費補助金(医療機器開発推進研究事業:身体機能解析・補助・代替機器開発研究事業)「高齢者の大腿骨頚部骨折等の治療を支援する高精度手術支援システム(H17-フィジ-一般-007)」によるものである．

6. 参考文献

1) 山路哲生, Dynamization の仮骨形成促進. 整形・災害外科 2002;Vol45(No4):p305－310.

Bone 45 (2009) 226–231

Contents lists available at ScienceDirect

Bone

journal homepage: www.elsevier.com/locate/bone

Prediction of proximal femur strength using a CT-based nonlinear finite element method: Differences in predicted fracture load and site with changing load and boundary conditions

Masahiko Bessho, Isao Ohnishi *, Takuya Matsumoto, Satoru Ohashi, Juntaro Matsuyama, Kenji Tobita, Masako Kaneko, Kozo Nakamura

Department of Orthopaedic Surgery, Faculty of Medicine, University of Tokyo, 7-3-1 Hongo, Bunkyo-ku, Tokyo 113-0033, Japan

ARTICLE INFO

Article history:
Received 12 June 2008
Revised 6 December 2008
Accepted 16 April 2009
Available online 3 May 2009

Edited by: J. Kanis

Keywords:
Osteoporosis
Hip fracture
Finite element method
CT
Bone strength

ABSTRACT

The annual occurrence of hip fracture due to osteoporosis as of 2002 had reached 120,000 in Japan. The increase has been very rapid. From a biomechanical perspective, hip fractures are thought to be caused in real settings by different directions of loading. Thus, clarification of the loading directions under which the proximal femur is most vulnerable to fracture would be helpful for elucidating fracture mechanics and establishing preventive interventions. The purpose of the current study was to clarify the influence of loading direction on strength and fracture site of the proximal femur using the CT-based nonlinear FE method to determine loading directions under which the proximal femur is most vulnerable to fracture. Contralateral femora were analyzed in 42 women with hip fracture (mean age, 82.4 years), comprising 20 neck fractures and 22 trochanteric fractures. Within 1 week after fracture, quantitative CT of the contralateral femur was performed in each patient and 3-dimensional FE models were created. One stance loading configuration (SC) and four different fall loading configurations (FC) were assigned. Nonlinear FE analysis was performed. Differences in fracture loads depending on differences in loading direction were analyzed and correlations among fracture loads in different loading directions were assessed. Next, fracture sites were also analyzed. Mean predicted fracture load in the SC was 3150 N. Mean fracture loads were 2270 N in FC1, 1060 N in FC2, 980 N in FC3, and 710 N in FC4. The correlation between predicted fracture loads in SC and those in each FC was significant with a correlation coefficient of 0.467–0.631. Predicted fracture sites in the SC appeared at the subcapital region in all patients and were categorized as neck fracture. However, trochanteric fractures occurred in all fall configurations except FC1. In FC1, a significant correlation was seen between real fracture type and predicted type. The current investigation could contribute to the acquisition of useful knowledge allowing the establishment of more efficacious means of preventing hip fractures.

Introduction

The annual occurrence of hip fracture due to osteoporosis as of 2002 had reached 120,000 in Japan. In Japan, the increase has been very rapid, with a 1.7-fold increase from 1987 to 1992 and a 2.2-fold increase from 1987 to 2002 [1]. More than 90% of fractures were reportedly caused by falls from standing height [2,3]. However, some cases display no clear evidence of falls or trauma [3,4]. From a biomechanical perspective, hip fractures are thought to be caused in real settings by different directions of loading. Thus, clarification of the loading directions under which the proximal femur is most vulnerable to fracture would be helpful for elucidating fracture mechanics and establishing preventive interventions.

Pinilla et al. [5] and Fujii [6] investigated the influence of loading direction on fracture load of the proximal femur. The results of these studies were derived by conducting compression testing of proximal femoral specimens obtained from excised cadaveric femora. One limitation of these studies was that only one load direction could be tested on one specimen and no other direction could be tested using the same specimen. To address this limitation, Ford et al. [7] and Keyak et al. [8] reported simulation studies on the influence of load direction using a computed tomography (CT)-based finite element (FE) method. However, those studies investigated strength of the excised femora and the analytical method was limited to a linear FE method. In addition, none of these studies examined fracture sites in detail. We have established our own CT-based nonlinear FE method to accurately predict fracture load and site on the proximal femur [9].

The purpose of the current study was to clarify the influence of loading direction on strength and fracture site of the proximal femur using the CT-based nonlinear FE method to determine loading directions under which the proximal femur is most vulnerable to fracture. In this study, validity of the FE method was also evaluated by analyzing strength and fracture site of the contralateral femur in

* Corresponding author. Fax: +81 3 3818 4082.
E-mail address: OHNISHII-DIS@h.u-tokyo.ac.jp (I. Ohnishi).

8756-3282/$ – see front matter © 2009 Elsevier Inc. All rights reserved.
doi:10.1016/j.bone.2009.04.241

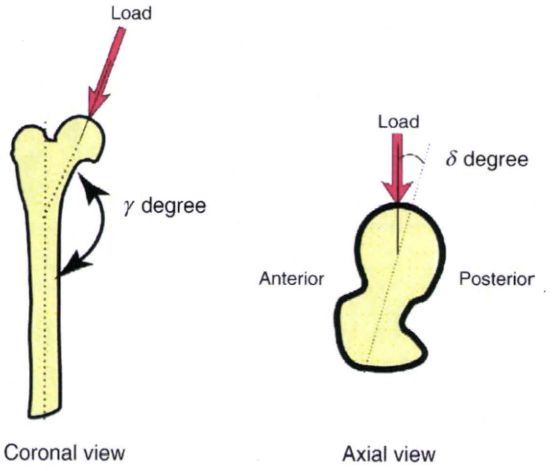

Fig. 1. Definition of the loading direction. Loading direction was defined as the angle γ with reference to the long axis of the femur in the frontal plane and δ with reference to the femoral neck axis in the horizontal plane. Left: coronal plane, right: axial plane.

patients with hip fracture, through which we examined whether our FE method could create fracture in the contralateral femur identical to the real fracture in the patient.

Patients and methods

Contralateral femora were analyzed in 42 women with hip fracture (mean age, 82.4 years; range, 70–92 years; mean height: 146 cm; mean weight: 44 kg), comprising 20 neck fractures (mean age, 81.9 years; mean height: 147 cm; mean weight: 45 kg) and 22 trochanteric fractures (mean age, 82.9 years; mean height: 146 cm; mean weight: 44 kg). No significant differences were seen in mean age ($p=0.60$), height ($p=0.68$) or weight ($p=0.72$). Fifty-three female patients with hip fracture were admitted to the University of Tokyo Hospital between January 2006 and December 2006. These included 4 patients with high-energy injury, 1 with a previous history of cancer, 3 who had received treatment with glucocorticoids, and 3 with metallic implants within the CT scan area. Therefore, after excluding these 11 patients, 42 patients were included in the present study. All patients had sustained fracture by a fall from standing height. All of them approved this study protocol after providing informed consent (initially verbal, later confirmed in writing). With the approval of the ethics committee in our hospital, all the following procedures were performed. Within 1 week after fracture, quantitative CT of the contralateral femur was performed in each patient and 3-dimensional FE models were created. Femora underwent CT using a calibration phantom and a slice thickness of 3 mm from the femoral head to the 17 cm below the minor trochanter (Aquilion Super 4; Toshiba Medical Systems, Japan; 120 kV, 75 mAs, pixel space, 0.625 mm; 512×512 matrix). From the CT data, FE models were created using triangular shell elements with a thickness of 0.4 mm and a size of 3 mm for the outer surface of the cortical bone and tetrahedral solid elements with a size of 3 mm for the rest of the bone [9]. The mean number of solid elements was 80,850, while the mean number of shell elements was 4794. To allow for bone heterogeneity, mechanical properties of each element were computed from the Hounsfield unit value. Ash density was approximated as equivalent to hydroxyapatite density, which neglects the effect of fat content on the Hounsfield unit value for trabecular bone [10–12]. Ash density for each voxel was determined from the linear regression equation derived by relating the Hounsfield unit of a calibration phantom to the equivalent ash density. Bone density of an element was determined from the mean number of Hounsfield units obtained for a total of 17 points in the element [9]. Young's modulus and yield stress of each tetrahedral element were calculated using the equations proposed by Keyak et al. [13] and Keller [14]. Poisson's ratio for each element was set as 0.4 [13]. In previous studies, Young's modulus of the cortex has been found to range from 11 to 24 GPa [15] or from 9 to 21 GPa [16]. Young's modulus of each triangular shell element was set as equivalent to that of the adjacent tetrahedral element located underneath the shell element, while the minimum Young's modulus of the shell element was set as 10 GPa.

Nonlinear FE analysis was performed using the Newton–Raphson method. To allow for the nonlinear phase, mechanical properties of

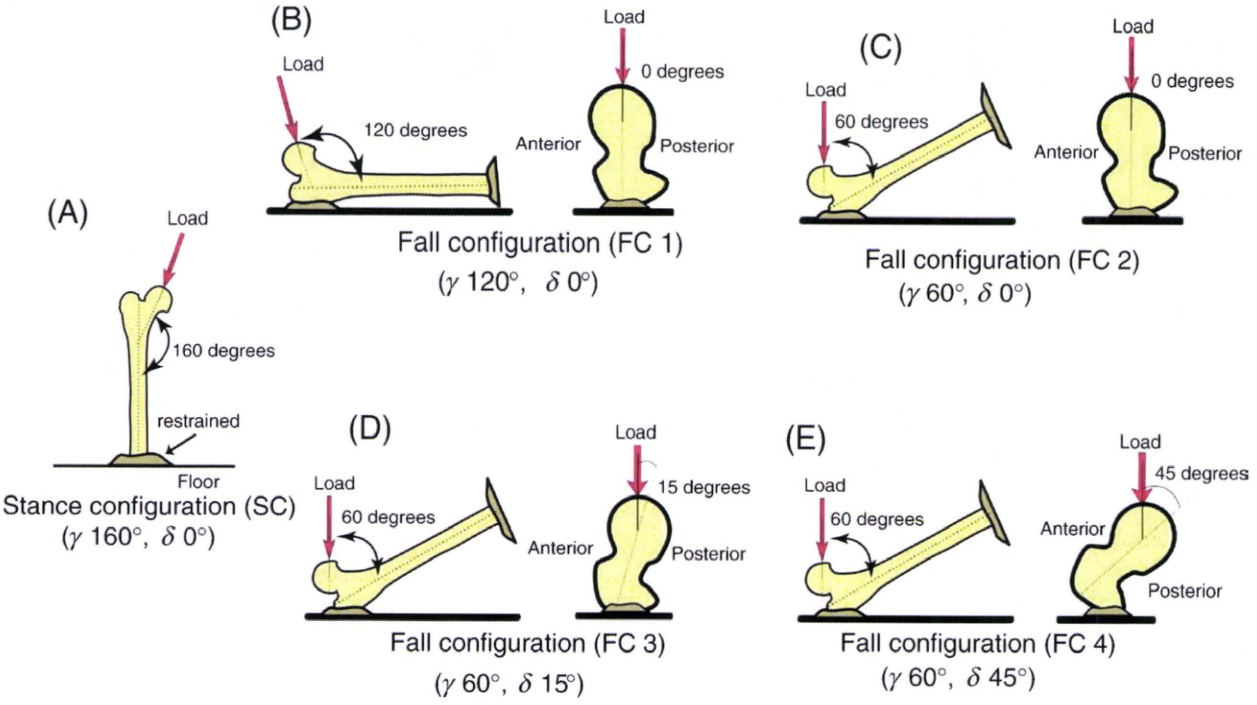

Fig. 2. Loading and boundary conditions. (A) Stance configuration. (B) Fall configuration 1 (FC1). (C) Fall configuration 2 (FC2). (D) Fall configuration 3 (FC3). (E) Fall configuration 4 (FC4).

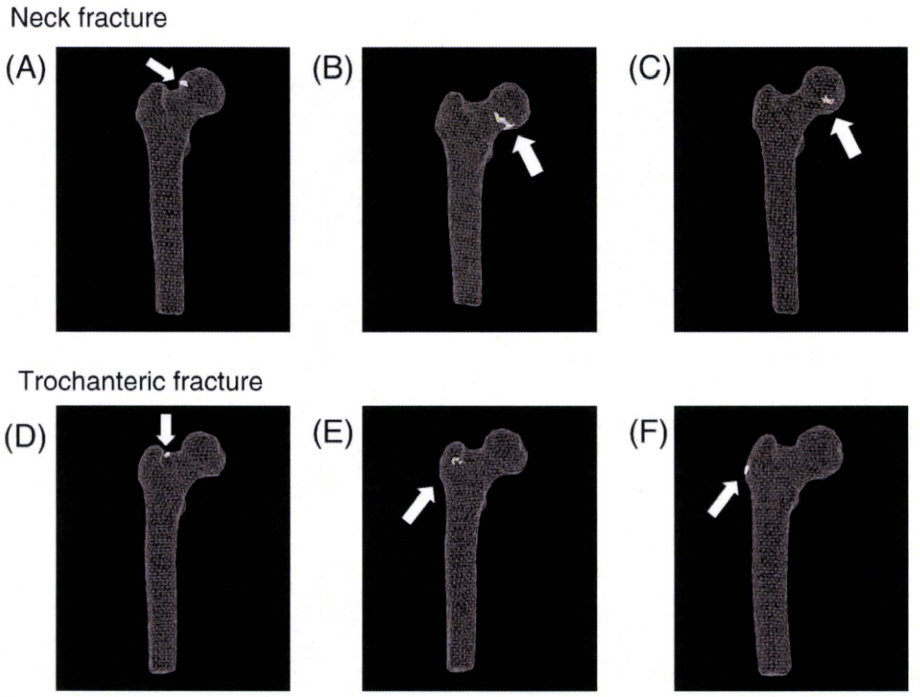

Fig. 3. Fracture types corresponding to each of the predicted fracture sites. Arrow: Predicted fracture site. (A) (B) (C) With predicted fracture sites located at the subcapital region, the type was classified as neck fracture. (D) With predicted fracture sites at the base of the femoral neck, the type was classified as trochanteric. (E) (F) With predicted fracture sites on the trochanteric region, the type was classified as trochanteric.

the elements were assumed to be bi-linear elastoplastic, and the post-yield modulus was set as 5% of E (where E is the pre-yield Young's modulus). The ratio of element ultimate stress to yield stress was assigned as 0.8. The element crack in tension was defined as occurring when maximum principal stress exceeded element ultimate stress. However, we introduced both yield and failure in compression. Yield in compression was defined as occurring when Drucker–Prager equivalent stress exceeded element yield stress. Element failure in compression was then defined as occurring when the negative value of maximum principal strain exceeded 10,000 microstrain. Fracture load was defined as the load when ≥1 shell element failed [9].

Loading direction was defined as the angle γ with reference to the long axis of the femur in the frontal plane and δ with reference to the femoral neck axis in the horizontal plane (Fig. 1) [8]. Angles $\gamma = 160°$ and $\delta = 0°$ were assigned as stance configuration (SC). For fall loading configuration, four different loading configurations were assigned. Fall configuration (FC) 1 used $\gamma = 120°$ and $\delta = 0°$. FC2 used $\gamma = 60°$ and $\delta = 0°$. FC3 used $\gamma = 60°$ and $\delta = 15°$. Likewise, FC4 used $\gamma = 60°$ and $\delta = 45°$ (Fig. 2) [6–8].

Differences in fracture loads depending on differences in loading direction were analyzed and correlations among fracture loads in different loading directions were assessed. Next, fracture sites were also analyzed. The predicted fracture type in the FE method was defined as follows. When initial failure of the triangular shell element occurred at a subcapital region, neck fracture was defined. Likewise, if initial failure of the shell element appeared at the basal neck or trochanteric region, trochanteric fracture was defined. The fracture types corresponding to the predicted fracture sites are shown in Fig. 3. Predicted fracture types were compared to the real fracture of the contralateral side in each patient.

Statistical analyses were performed using Pearson's test, Fisher's exact test and Friedman test. Scheffe's test was also utilized for post hoc testing. Values of $p<0.05$ were considered statistically significant.

Results

Mean (±standard deviation (SD)) predicted fracture load in the SC was 3150±611 N. Mean fracture loads were 2270±600 N in FC1, 1060±248 N in FC2, 980±229 N in FC3, and 710±174 N in FC4 (Fig. 4). Mean predicted fracture load was significantly larger than in the SC than in all FCs except FC1 ($p<0.001$). To compare mean fracture loads among FCs, the load in FC1 was significantly larger than those of FC2, FC3 and FC4 ($p<0.01$, $p<0.001$, $p<0.001$,

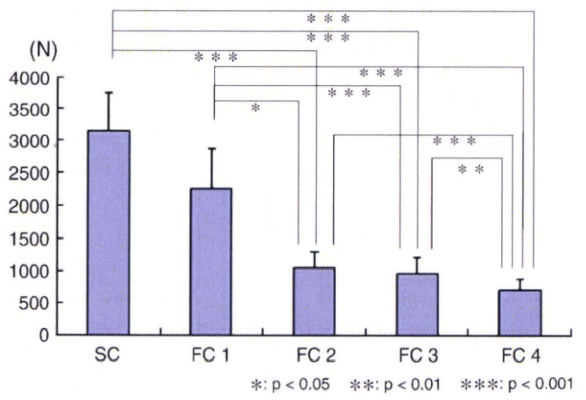

Fig. 4. The mean predicted fracture loads for each configuration. The *X* axis indicates load and boundary conditions and the *Y* axis indicates predicted strength. SC: Stance configuration, FC: fall configuration.

Table 1
Correlations (r) of the predicted fracture loads for each loading configuration.

	SC	FC1	FC2	FC3	FC4
SC	–	0.467**	0.615***	0.614***	0.631***
FC1	0.467**	–	0.586***	0.584***	0.463**
FC2	0.615***	0.586***	–	0.894***	0.728***
FC3	0.614***	0.584***	0.894***	–	0.861***
FC4	0.631***	0.463**	0.728***	0.861***	–

** $p<0.01$.
*** $p<0.001$.

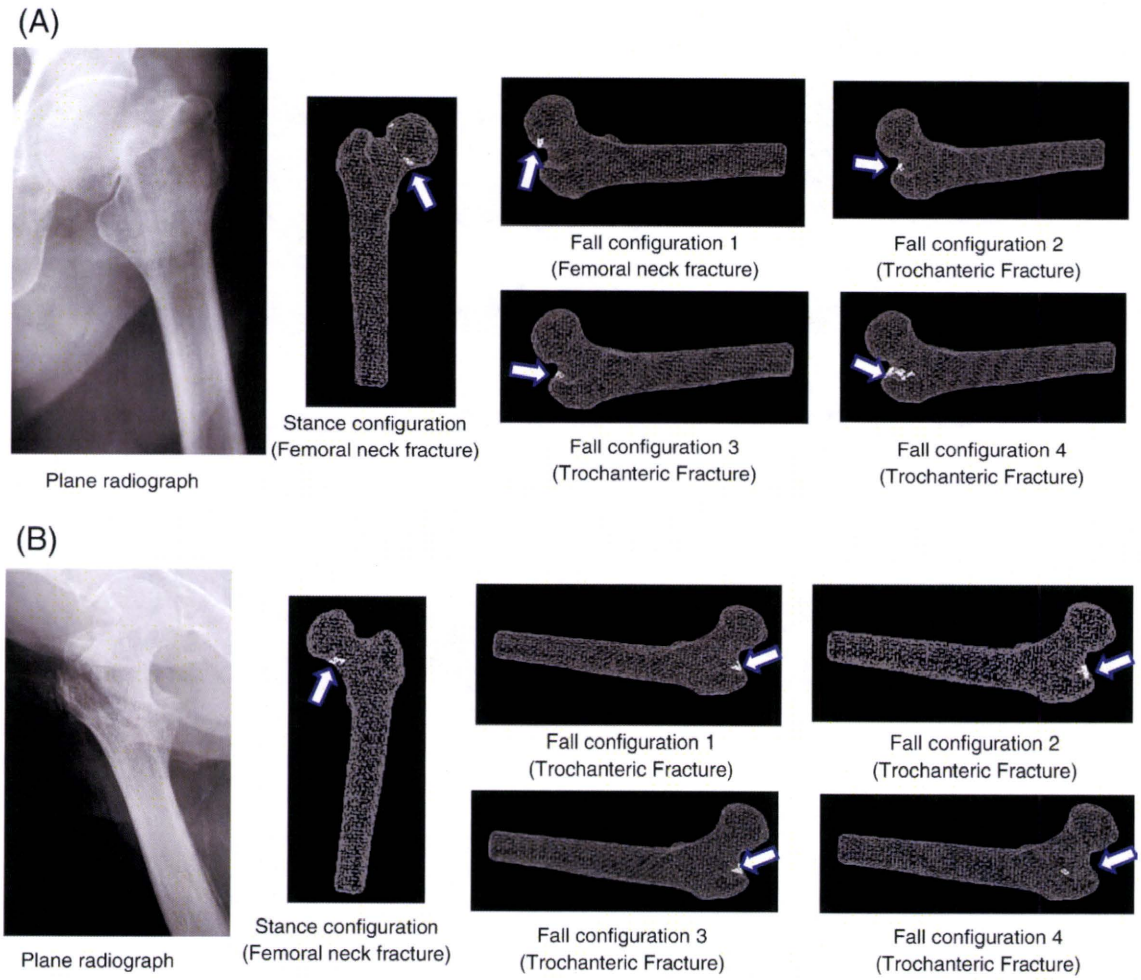

Fig. 5. The predicted fracture sites for each configuration. The shell elements in failure are shown on the 3 dimensional finite element model. Arrow: The predicted fracture site. Words in parentheses: the predicted fracture type. (A) 89 years old (femoral neck fracture, Garden classification, Stage IV) (B) 83 years old (trochanteric fracture, Evans classification Type I, group 2).

respectively). Load was significantly larger in FC2 than in FC4 ($p<0.001$). Likewise, load was significantly larger in FC3 than in FC4 ($p<0.01$).

Correlation coefficients of predicted fracture load among all configurations are listed in Table 1. The correlation coefficient relating the predicted strength under SC to that under FC1 was 0.467 (95% confidence interval: 0.190–0.675, $p=0.0016$). The coefficient relating SC to FC2 was 0.615 (95% confidence interval: 0.383–0.775, $p<0.0001$). The coefficient relating SC to FC3 was $r=0.615$ (95% confidence interval: 0.383–0.775, $p<0.0001$). The coefficient relating SC to FC4 was $r=0.631$ (95% confidence interval: 0.405–0.785, $p<0.0001$). The coefficient relating FC1 to FC2 was $r=0.586$ (95% confidence interval: 0.344–0.756, $p<0.0001$). The coefficient relating FC1 to FC3 was $r=0.584$ (95% confidence interval: 0.340–0.754, $p<0.0001$). The coefficient relating FC1 to FC4 was $r=0.463$ (95% confidence interval: 0.185–0.672, $p=0.0017$). The coefficient relating FC2 to FC3 was $r=0.894$ (95% confidence interval: 0.810–0.942, $p<0.0001$). The coefficient relating FC2 to FC4 was $r=0.728$ (95% confidence interval: 0.545–0.845, $p<0.0001$). The coefficient relating FC3 to FC4 was $r=0.861$ (95% confidence interval: 0.755–0.923, $p<0.0001$).

All predicted fracture sites could be categorized by the failure of shell elements into two types, namely neck fractures and trochanteric fractures (Fig. 5). Predicted fracture sites in the SC appeared in the subcapital region in all patients and were categorized as neck fractures. However, trochanteric fractures occurred in all fall configurations except FC1. In FC1, both the neck and trochanteric fractures occurred, with 16 neck fractures in 20 patients with contralateral neck fracture and 18 trochanteric fractures in 22 patients with contralateral trochanteric fractures. A significant correlation was seen between real fracture type and predicted type ($p<0.001$) (Table 2).

Discussion

From the results of our study, the predicted strength under the loading condition simulating a fall in the posterolateral direction was smaller than that by a fall in the lateral direction. These results were consistent with those of a previous study that conducted mechanical testing using cadaveric specimens [6] and predicted strength using a CT/FEM [7,8].

Table 2
The predicted fracture types for each loading configuration and each fracture type.

Conditions	SC		FC1		FC2		FC3		FC4	
The predicted fracture type	N	T	N	T	N	T	N	T	N	T
Patients with femoral neck fracture ($n=20$)	20	0	16	4	0	20	0	20	0	20
Patients with trochanteric fracture ($n=22$)	22	0	4	18	0	22	0	22	0	22

Predicted fracture sites in the SC appeared in the subcapital region in all patients and were categorized as neck fractures. However, trochanteric fractures occurred in all fall configurations except FC1. In FC1, both the neck and trochanteric fractures occurred, with 16 neck fractures in 20 patients with contralateral neck fracture and 18 trochanteric fractures in 22 patients with contralateral trochanteric fractures. N: femoral neck fracture, T: trochanteric fracture.

The magnitude of strength of the proximal femur under a certain loading condition differs depending on the bone density distribution and morphology of each individual patient. To evaluate fracture risk in each patient, it is ideal to analyze strengths under all loading conditions occurring in the activities of daily living. However, it takes a large amount of time to carry out predictions as a screening using CT/FEM under many circumstances. One of the solutions to this problem is to find the typical loading direction that correlates with other conditions. For this reason, we investigated the correlation among multiple loading conditions. The correlation between predicted fracture loads in SC and those in each FC was significant but weak, with a correlation coefficient of 0.467–0.631. To evaluate strength of the proximal femur in each individual patient, both strength under SC and strength under FC should be assessed. The correlations of the predicted strength among FC2, FC3, and FC4 were relatively high with correlation coefficients of 0.728 to 0.894. Upon further analysis of these conditions, the correlation coefficients were even higher with 0.894 between FC3 and FC2 and 0.861 between FC3 and FC4. Thus, FC3 was thought to be representative of FC2 and FC4. Conversely, the predicted strength under FC1 had poor correlations between FC2, FC3, and FC4 with coefficients of 0.586, 0.584, and 0.463 respectively. Thus, it was concluded that the strength under FC1 should be evaluated independently.

In all FCs except FC1, only trochanteric fractures were predicted. However, in FC1, both neck and trochanteric fractures were predicted. Hirsch and Frankel [17] reported that compressive force along the long axis of the neck is necessary to cause femoral neck fracture. Femoral neck angle is reportedly 120–130° [18]. FC1 may thus be able to cause femoral neck fractures. Fujii also reported that FC1 generated neck fractures and that this does not contradict the results of previous studies [6]. Hall et al. reported that the difference in bone density between the right and left femora as measured by dual X-ray absorptiometry was within 5% and that it was sufficient for measuring either side of the femur to evaluate osteoporosis [19]. Boston [20] reported that in 83% of the patients with previous hip fracture who sustained another hip fracture on the contralateral side, the fracture type agreed well with the previous one. If morphological differences between both sides of the femur are assumed to be absent, loading direction alone appears to represent the decisive factor for fracture type under all FCs except FC1. However, the different fracture type in FC1 could be generated by differences in morphology of the proximal femur in each individual patient.

Ford et al. [7] and Keyak et al. [8] investigated the influence of load direction on strength of the proximal femur. Ford et al. and Keyak et al. reported that the predicted strength by CT/FEM tended to decrease as the loading direction shifted from lateral to posterolateral. This was not contradictory to our findings. However, the analytical method adopted in those studies was a linear finite element method and the number of analyzed materials was only one sample in the study by Ford et al. and four samples in the study by Kayak et al. For this reason, they did not conduct the statistical analysis that we did. In addition, neither of these studies evaluated fracture site or type.

The load and boundary conditions adopted in the present study did not include muscle forces or reaction forces generated from ligamentous attachments. In addition, analyses utilized static mechanics rather than impact mechanics. Shock absorption by the soft tissues of patients was not taken into account [21]. Conditions in the simulation thus differed from those in actual settings. However, the load and boundary conditions adopted in the study were thought to reflect actual conditions, as simulated fractures resembled those sustained by the subjects. Further investigation adopting more realistic conditions is necessary, to take into account muscle forces and reaction forces from ligaments. Another limitation in this particular simulation technique was the inability to deal with large deformation of the model, from which refracture of bone fragments by collision could be simulated. The current method could only detect the initial failure site of the element under small deformation of the model, as although the results showed that fracture type could be judged even using this technique.

Previous studies have investigated the strengths of specimens ex vivo, whereas our study investigated strengths of the proximal femur in patients. In CT of the proximal femur in patients, images may have been deteriorated due to the influence of the pelvis or soft tissues nearby. Accuracy of strength prediction in vivo using a CT-based FE method could thus be impaired. Keyak and Falkinstein compared predicted strengths using a CT-based FE method from CT data obtained from two cadaveric specimens in situ to those from the same specimens in vitro [22]. Prediction from in situ specimens was found to overestimate strength by 8–13%. Although our study adopted a different simulation method from that of Keyak et al., our results might still have overestimated strength. However, our simulation method minimized partial volume effects by using triangular elements on the outer surface of the model. In addition, bone mineral density in tetrahedral elements was determined from mean value in Hounsfield units at 17 points within the element, to accurately simulate the distribution of bone mineral density even when the quality of CT data might have been deteriorated.

Our aim was to provide a quantitative diagnostic tool to accurately evaluate bone fracture risk by taking as many determinant factors for bone strength as possible into consideration. The CT-based FEM is the most advanced method to satisfy these demands. Our intention was not to provide a method to decide whether a bone in a certain patient would break under a certain mechanical environment. Instead, our approach involved the virtual extraction of a bone of interest from a patient and examining it under virtual static mechanical testing. The predicted strength from this simulation may be far from accurate in comparison to that derived from more realistic simulations incorporating dynamic analyses or more realistic mechanics incorporating geometrical rigidity/nonlinearity. Despite these limitations, the CT-based FEM offers a far more advanced method to diagnose bone fragility than the prevailing clinically available bone densitometry. Our model predicts elements where failure initiates, but does not take large deformation/geometrical nonlinearity into consideration. Our previous study verifying the accuracy of predicted fracture site by FEM simulation disclosed that the predicted fracture sites agreed well with the experimental fracture sites [9]. In the future, we intend to adopt more advanced simulation methods, including dynamic analyses or buckling simulations incorporating large deformation analyses or analyses with geometrical rigidity/nonlinearity.

To investigate the discrimination power of the CT/FEM, it is necessary to conduct a case-controlled study investigating the sensitivity and specificity of the CT/FEM by comparing the predicted strengths between patients with fractures and patients without fractures. However, the present study was not aimed at investigating the above issues. We clarified the loading directions that are vulnerable to fracture in the patients with hip fracture and the results were not contradictory to those of previous studies. Because a case-controlled study involving patients without fractures is also proceeding in our department, the results from this comparative study will soon be reported. If we could identify the loading directions under which the proximal femur is most vulnerable to fracture, more effective means of preventing fracture might be identified. With such knowledge, shape or attachment site of hip protectors could be optimized to maximize fracture prevention [23]. Likewise, motion exercises could be provided for elderly individuals to avoid falls in the most risky directions. The current investigation could contribute to the acquisition of useful knowledge allowing the establishment of more efficacious means of preventing hip fractures.

Acknowledgments

This work was funded by a grant in aid for Scientific Research received from the Japan Society for the Promotion of Science (14657356).

References

[1] Yoshimura N, Suzuki T, Hosoi T, Orimo H. Epidemiology of hip fracture in Japan: incidence and risk factors. J Bone Miner Metab 2005;23:78–80 Suppl.
[2] Hedlund R, Lindgren U. Trauma type, age, and gender as determinants of hip fracture. J Orthop Res 1987;5:242–6.
[3] Cummings SR, Black DM, Nevitt MC, Browner WS, Cauley JA, Genant HK, et al. Appendicular bone density and age predict hip fracture in women. The Study of Osteoporotic Fractures Research Group. JAMA 1990;263:665–8.
[4] Sloan J, Holloway G. Fractured neck of the femur: the cause of the fall? Injury 1981;13:230–2.
[5] Pinilla TP, Boardman KC, Bouxsein ML, Myers ER, Hayes WC. Impact direction from a fall influences the failure load of the proximal femur as much as age-related bone loss. Calcif Tissue Int 1996;58:231–5.
[6] Fujii M. Experimental study on the mechanism of femoral neck fractures. Nippon Seikeigeka Gakkai Zasshi 1987;61:531–41.
[7] Ford CM, Keaveny TM, Hayes WC. The effect of impact direction on the structural capacity of the proximal femur during falls. J Bone Miner Res 1996;11: 377–83.
[8] Keyak JH, Skinner HB, Fleming JA. Effect of force direction on femoral fracture load for two types of loading conditions. J Orthop Res 2001;19:539–44.
[9] Bessho M, Ohnishi I, Matsuyama J, Matsumoto T, Imai K, Nakamura K. Prediction of strength and strain of the proximal femur by a CT-based finite element method. J Biomech 2007;40:1745–53.
[10] Ito M, Lang TF, Jergas M, Ohki M, Takada M, Nakamura T, et al. Spinal trabecular bone loss and fracture in American and Japanese women. Calcif tissue int 1997;61: 123–8.
[11] Keyak JH, Kaneko TS, Rossi SA, Pejcic MR, Tehranzadeh J, Skinner HB. Predicting the strength of femoral shafts with and without metastatic lesions. Clin Orthop Relat Res 2005;439:161–70.
[12] Keyak JH, Kaneko TS, Tehranzadeh J, Skinner HB. Predicting proximal femoral strength using structural engineering models. Clin Orthop Relat Res 2005:219–28.
[13] Keyak JH, Rossi SA, Jones KA, Skinner HB. Prediction of femoral fracture load using automated finite element modeling. J Biomech 1998;31:125–33.
[14] Keller TS. Predicting the compressive mechanical behavior of bone. J Biomech 1994;27:1159–68.
[15] Bayraktar HH, Morgan EF, Niebur GL, Morris GE, Wong EK, Keaveny TM. Comparison of the elastic and yield properties of human femoral trabecular and cortical bone tissue. J Biomech 2004;37:27–35.
[16] McCalden RW, McGeough JA, Barker MB, Court-Brown CM. Age-related changes in the tensile properties of cortical bone. The relative importance of changes in porosity, mineralization, and microstructure. J Bone Joint Surg 1993;75-A: 1193–205.
[17] Hirsch C, Frankel VH. Analysis of forces producing fractures of the proximal end of the femur. J Bone Joint Surg Br 1960;42:633–40.
[18] Anderson JY, Trinkaus E. Patterns of sexual, bilateral and interpopulational variation in human femoral neck-shaft angles. J Anat 1998;192(Pt 2):279–85.
[19] Hall ML, Heavens J, Ell PJ. Variation between femurs as measured by dual energy X-ray absorptiometry (DEXA). Eur J Nucl Med 1991;18:38–40.
[20] Boston DA. Bilateral fractures of the femoral neck. Injury 1982;14:207–10.
[21] Robinovitch SN, McMahon TA, Hayes WC. Force attenuation in trochanteric soft tissues during impact from a fall. J Orthop Res 1995;13:956–62.
[22] Keyak JH, Falkinstein Y. Comparison of in situ and in vitro CT scan-based finite element model predictions of proximal femoral fracture load. Med Eng Phys 2003;25:781–7.
[23] Wiener SL, Andersson GB, Nyhus LM, Czech J. Force reduction by an external hip protector on the human hip after falls. Clin Orthop 2002:157–68.

SPINE Volume 34, Number 14, pp 1464–1469

Prediction of Vertebral Strength Under Loading Conditions Occurring in Activities of Daily Living Using a Computed Tomography-Based Nonlinear Finite Element Method

Takuya Matsumoto, MD,* Isao Ohnishi, MD, PhD,* Masahiko Bessho, MD, PhD,* Kazuhiro Imai, MD, PhD,*† Satoru Ohashi, MD,* and Kozo Nakamura, MD, PhD*

Study Design. A clinical study on osteoporotic vertebral strength in daily living using a computed tomography (CT)-based nonlinear finite element (FE) model.

Objective. To evaluate the differences in predicted fracture strength of osteoporotic vertebral bodies among the different loading conditions that are occurring in the activities of daily living.

Summary of Background Data. FE model has been reported to predict vertebral strength in uniaxial loading, but forward bending load plays an important role in osteoporotic vertebral fractures.

Methods. Strengths of the second lumbar vertebra in 41 female patients with postmenopausal osteoporosis were analyzed using a nonlinear CT-based FE method. Three different loading conditions were adopted uniaxial compression, forward bending, and erect standing. The same boundary condition was used for all loading conditions. Predicted strengths under forward bending and erect standing were compared with that under uniaxial compression and differences in strength were statistically analyzed.

Results. The regression equation relating strength under uniaxial compression to that under erect standing was expressed as $y = 0.8912x + 19.332$ ($R = 0.9522$), whereas the equation relating uniaxial compression to forward bending was $y = 0.7033x + 55.071$ ($R = 0.8342$). Both relationships were significant, but the correlation between forward bending and uniaxial compression was not strong, while strength was lower under forward bending than under uniaxial compression according to the Friedman multiple comparison test ($P = 0.00017$).

Conclusion. Strength under forward bending correlated significantly to that under uniaxial compression, but the correlation was not strong. Therefore, in osteoporotic patients, both uniaxial compression and forward bending should be assessed to evaluate fracture risk in daily living using a CT-based FE method.

Key words: vertebral fracture, osteoporosis, fracture strength prediction, nonlinear finite element analysis, fracture site. **Spine 2009;34:1464–1469**

From the *Department of Orthopaedic Surgery, University of Tokyo, Tokyo, Japan; and †Department of Orthopaedic Surgery, Tokyo Metropolitan Geriatric Medical Center, Tokyo, Japan.

Acknowledgment date: June 17, 2008. Revision date: January 17, 2009. Acceptance date: January 19, 2009.

The manuscript submitted does not contain information about medical device(s)/drug(s).

No funds were received in support of this work. No benefits in any form have been or will be received from a commercial party related directly or indirectly to the subject of this manuscript.

Address correspondence and reprint requests to Isao Ohnishi, MD, PhD, Department of Orthopaedic Surgery, School of Medicine, Tokyo University, 7-3-1 Hongo, Bunkyo-ku, Tokyo 113-0033, Japan; E-mail: ohnishii-dis@h.u-tokyo.ac.jp

Osteoporosis is a disease characterized by low bone mass and microarchitectual deterioration of bone tissue, leading to enhanced bone fragility and a resulting increase in fracture risk.[1] Osteoporotic vertebral fracture is common in the elderly, representing a serious event causing reduced activity or bedridden status with high mortality and morbidity rates.

Osteoporotic vertebral fractures occasionally occur slowly and asymptomatically and tend to be overlooked by clinicians. Such fractures seem to be caused by loading on the spine during activities of daily living that exceed the vertebral strength of the osteoporotic individual.[2] The most common type of vertebral fracture is reportedly wedge-shaped fracture[3,4] caused by axial and bending loads.[5,6] To assess the strength of osteoporotic vertebrae, evaluating vertebral strength under loading as experienced during daily living is important, particularly forward bending. Bone densitometry techniques can neither predict differences in bone strength with changing load direction nor identify sites at risk of fracture. Finite element models (FEM) based on data from quantitative computed tomography may predict vertebral strength more accurately because geometry, architecture, and heterogeneous mechanical properties of the bone are assessed. We have previously reported that vertebral strength could be predicted accurately using a computed tomography (CT)-based nonlinear FE method.[7] This method can also be used for *in vivo* assessments of vertebral strength.[8] Once accuracy has been established, various simulations will be able to be used in other situations by changing the direction and/or site of loading. If we could create a patient-specific CT-based nonlinear FE model of the vertebral body and strengths could be predicted under loading conditions simulating common activities of daily living, this would provide an extremely useful tool in clinical practice. On this background, we focused on the use of simulated loading conditions that are commonly encountered during activities of daily living. The purpose of the present study was to evaluate differences in predicted fracture strength of vertebral bodies among different loading conditions occurring during activities of daily living. Based on these analyses, we may be able to determine whether multiple loading conditions are necessary to evaluate vertebral fracture risk in osteoporotic persons.

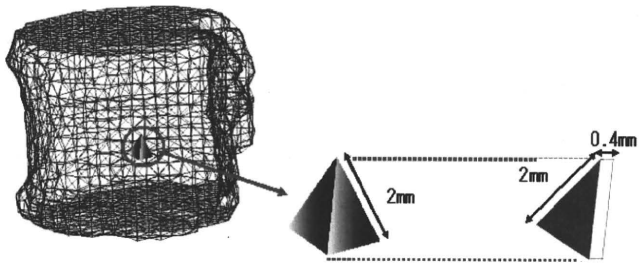

Figure 1. A FEM of a whole vertebral body. Trabecular bone was simulated using 2-mm tetrahedron elements, and the cortical shell was modeled using 2-mm triangular plates with a thickness of 0.4 mm. This model consisted of 4437 tetrahedral elements and 2518 triangular shell elements on average.

■ Materials and Methods

Subjects comprised 41 female patients (mean age, 69.4 years; range: 51–88 years) who could walk, visited the outpatient clinic of the Department of Orthopedic Surgery at the University of Tokyo between 2005 and 2007 and were diagnosed as postmenopausal osteoporosis according to the guidelines for prevention and treatment of osteoporosis as proposed by the Japanese Society of Osteoporosis (2006 ed.). No subjects had any previous history of disease or use of drugs affecting bone metabolism. The second lumbar vertebra (L2) was examined in these patients, and subjects with previous L2 fracture were excluded. With ethics committee approval, CT of L2 was performed after obtaining informed consent from each patient. CT of L2 was obtained using a slice thickness of 2 mm[8] and a pixel width of 0.37 mm with an Aquilion system (Toshiba Medical Systems, Tokyo, Japan; 120 kV, 75 mAs, 512 × 512 matrix), as along with a calibration phantom (B-MAS200; Kyoto Kagaku, Kyoto, Japan) containing 5 hydroxyapatite rods (0, 50, 100, 150, and 200 mg/cm^3). Predicted strengths under forward bending and erect standing were compared with that under uniaxial compression and differences in strength were statistically analyzed.

Nonlinear FE Analysis

Quantitative computed tomography-based FE models of vertebrae were created using methods described previously.[7–9] Mechanical Finder software, developed by the authors,[7–9] was used to extract bone area and for FE analyses. CT data in digital imaging and communication in medicine format were transferred to the workstation (Endeavor Pro-1000; Epson Direct, Nagano, Japan), and bone area of the L2 vertebral body was extracted from each scan. FE mesh models were then generated using the advancing front method. An FE model was created with 2-mm tetrahedral elements. Triangular elements with a thickness of 0.4 mm were attached to the model surface. On average, there were 44,337 tetrahedral elements and 2517 triangular shell elements (Figure 1).

To allow for bone heterogeneity, mechanical properties of each element were computed from the Hounsfield unit value. Ash density of each voxel was determined from the linear regression equation created by values from the calibration phantoms. Ash density of each element was set as the average ash density of voxels contained in one element. Young's modulus and yield stress of each tetrahedron element were calculated from the equations proposed by Keyak *et al.*[10] Young's modulus of cancellous tissue in human vertebrae has been reported as 3.8 to 13.4 GPa[11–14]; the minimum Young's modulus of each triangular plate was set as 10 GPa. Poisson's ratio of each element was set at 0.4, as used in previous articles.[7,9]

A uniaxial compressive load with uniform distribution was applied on the upper surface of the vertebra, with all elements and all nodes of the lower surface completely restrained. Loading configurations for erect standing and forward bending as described by Pollintine *et al*[15] were modified and adopted for analysis, as these were the postures most frequently occurring in the activities of daily living. Pollintine *et al* divided the loading area on the endplate of the vertebral body into 3 parts: anterior; posterior; and facet joint. They reported ratios of load magnitude (anterior: posterior: facet) of 19:41:40 for erect standing and 59:38:3 for forward bending. We modified the load distribution on the endplate according to these findings, as our model excluded posterior elements such as pedicles, lamina, and facet joints. Load distribution was divided into 3 parts: anterior; middle; and posterior. The ratio of load magnitude for each part was assigned on the assumption that the middle part bore the average load magnitude of the anterior and posterior parts. Ratios were thus 19:31:41 for erect standing and 59:48:38 for forward bending. Load was applied on the upper end plate vertically and the lower end plate was fully restrained (Figure 2).

Nonlinear analysis was performed using the Newton-Raphson method with a postyield modulus of 0.05. The ratio of ultimate stress to yield stress was assigned as 0.8. The element crack in tension was defined as occurring when maximum principal stress exceeded element ultimate stress. However, in compression, we introduced both yield and failure. Yield in compression was defined as occurring when Drucker-Prager equivalent stress exceeded element yield stress. Element failure in compression was then defined as occurring when the negative value of maximum principal strain exceeded 10,000 microstrain. Fracture load was defined as the load when at least one element failed. Predicted fracture load in each of the erect standing and forward bend-

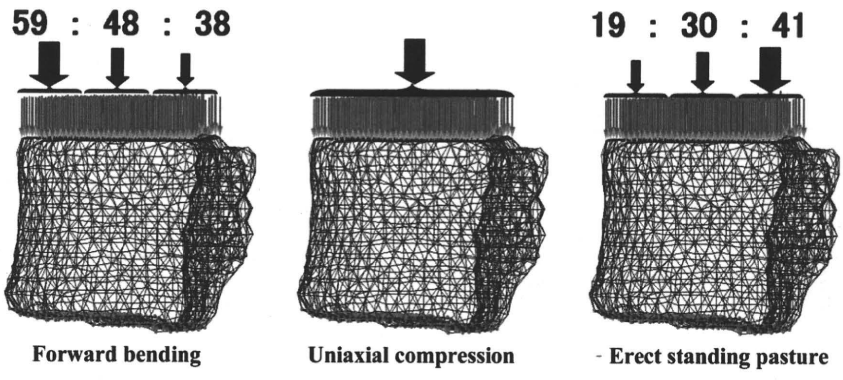

Figure 2. Load and boundary conditions in each model. Load distribution was divided into 3 parts: anterior; middle; and posterior. The ratio of load was thus 19:31:41 for erect standing and 59:48:38 for forward bending.

ing configurations was calculated and compared with that under uniaxial compression. To investigate differences among the 3 fracture loads from the different loading conditions, fracture load ratios were calculated. Fracture load ratio of forward bending (R_f) was represented as:

$$R_f = \frac{F_f}{F_u},$$

where F_f is predicted fracture load under forward bending and F_u is predicted fracture load under uniaxial compression.

Predicted fracture sites under each loading configuration were also identified. To analyze differences in distribution of fracture sites depending on differences in loading configuration, the whole vertebral body was divided into 3 parts in an anteroposterior direction and 3 parts in a cranio-caudal direction, for a total of 9 parts. Pearson correlation analyses were performed using StatView 5.0 (SAS Institute, Cary, NC). Paired analyses among the 3 groups were performed using the Friedman multiple comparison test. Analysis of differences in distributions of predicted fracture sites was performed using the χ^2 test for all loading conditions. Deviation of the distribution was analyzed by Ryan's method. Differences were considered significant for values of $P < 0.05$.

■ Results

Mean fracture load was 3062 N under uniaxial compression (range: 883–5688 N), 2918 N in erect standing (range: 883–5492 N), and 2693 N in forward bending (range: 883–5296 N). The linear regression equation relating fracture load in erect standing to that under uniaxial compression was expressed as y = 0.8912x + 19.332 (R = 0.9522, $P < 0.0001$) (Figure 3). Likewise, the equation relating forward bending to uniaxial compression was y = 0.7033x + 55.071 (R = 0.8342, $P < 0.0001$) (Figure 4). Mean fracture load was significantly lower in forward bending than under uniaxial compression ($P = 0.00017$).

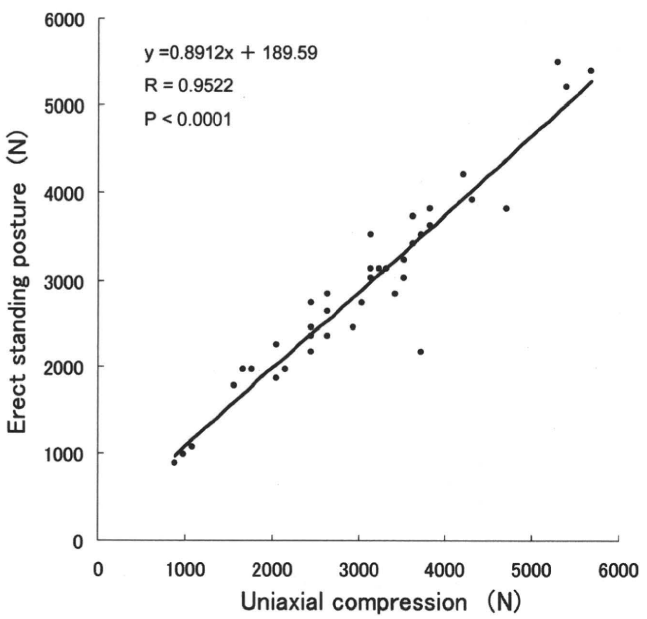

Figure 3. Predicted strengths under uniaxial loading and erect standing. A significant correlation was identified.

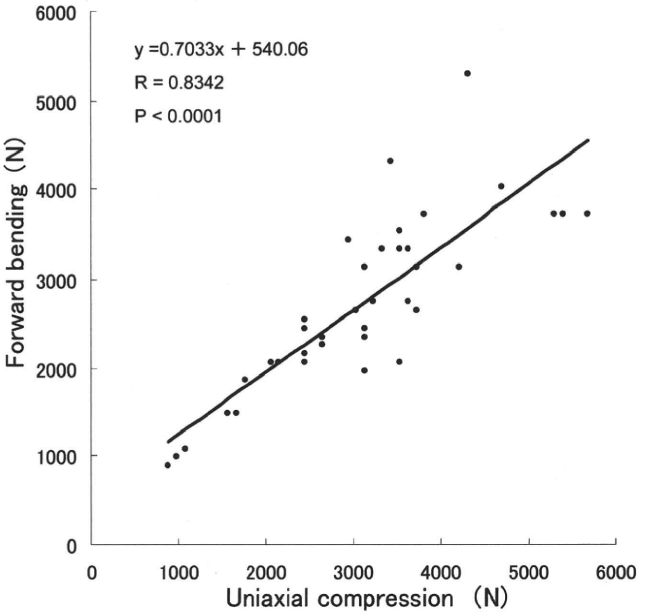

Figure 4. Predicted strengths under uniaxial loading and forward bending. A significant correlation was again identified.

In the evaluation of ratios of fracture load, as fracture load under uniaxial compression increased, fracture load ratio of both forward bending and erect standing tended to decrease (forward bending: y = −0.0527x + 1.0624, R = 0.393, $P = 0.0105$; erect standing: y = −0.0313x + 1.0617, R = 0.335, $P = 0.0137$) (Figure 5).

The distribution of predicted fracture sites is shown in Figure 6 for each of the loading configurations. In the cranio-caudal direction, fracture sites tended to be located in the upper third of the vertebral body under all loading configurations. In the anteroposterior direction, the antero-superior part was the most frequent predicted fracture site in forward bending, with76% of all sites. For both erect standing and uniaxial compression, the middle-superior part was the most frequent site (Figure 6). Under all loading conditions, significant differences existed in the distribution of predicted fracture sites. Using Ryan's multiple comparison, the antero-superior part was the most frequent fracture site in forward bending ($P < 0.005$). Under uniaxial loading, the middle-superior part was significantly more frequently affected than all parts except the antero-superior and postero-middle parts ($P < 0.005$). In erect standing, the middle-superior and postero-middle parts were significantly more frequent than the antero-middle and 3 inferior parts ($P < 0.005$) (Figure 7).

■ Discussion

Given the present results, fracture loads in erect standing and forward bending were highly correlated with those under uniaxial compression, with a correlation coefficient of 0.9522. However, the correlation between forward bending and uniaxial compression was moderate, with a coefficient of 0.8342. Strength in forward bending was significantly lower than uniaxial compression ac-

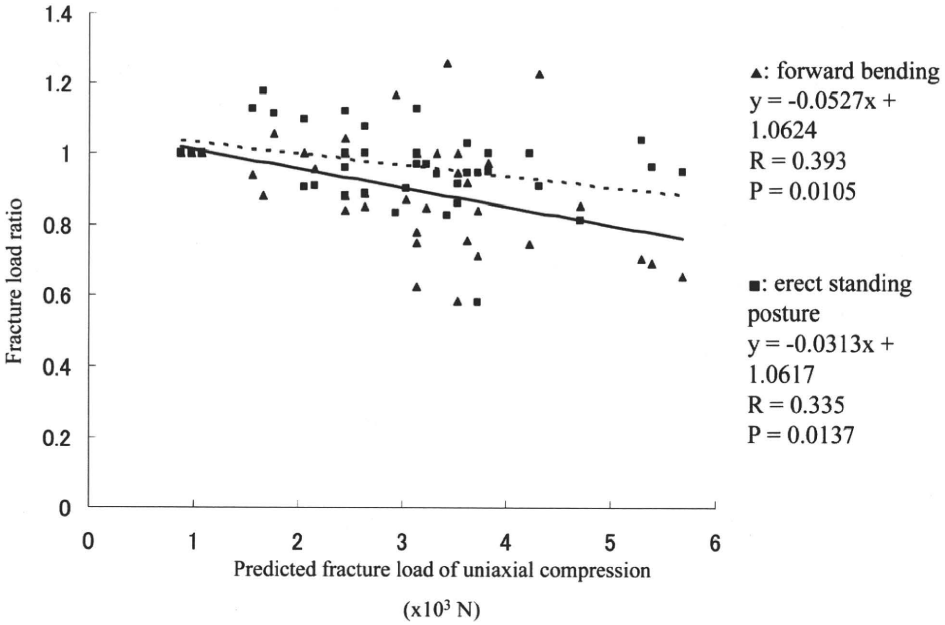

Figure 5. Fracture load ratio of forward bending to uniaxial compression (R_f) is represented as: $R_f = \frac{F_f}{F_u}$, where F_f is predicted fracture load of forward bending and F_u is predicted fracture load of uniaxial compression. As fracture load under uniaxial compression increased, the ratio tended to decrease. The correlation equation for the ratio of forward bending was $y = -0.0527x + 1.0624$ ($R = 0.393$, $P = 0.0105$). The correlation equation for the ratio of erect standing was $y = -0.0313x + 1.0617$ ($R = 0.335$, $P = 0.0137$).

cording to Friedman analysis. For fracture load ratio, as fracture load under uniaxial compression increased, the ratio of fracture load in forward bending to that under uniaxial compression tended to decrease. Therefore, when evaluating risk of vertebral fracture, assessment of predicted fracture load would need to be independently determined under each of the loading conditions to fully evaluate fracture risk during activities of daily living. Strength under uniaxial compression is clearly not representative of strengths under other loading configurations. If loading configurations under which the vertebrae are most vulnerable can be determined using CT-based FE analysis, atraumatic osteoporotic fractures may be able to be prevented by instructing patients to avoid such postures in activities of daily living.

Oda *et al*[16] reported that the most common deformity after atraumatic vertebral body fracture is a wedge-shaped deformity resulting from collapse of the anterior vertebral body. Wilke *et al*[17] reported that intradiscal pressure doubles with forward bending. A much larger compressive load is thus applied to the end plate during forward bending. Loading associated with forward bending was thought to be one of the factors causing wedge-shaped fracture, as the loading configuration that simulated forward bending in our study created identical wedge-shaped deformities of the vertebral body. Conversely, under erect standing and uniaxial compression, predicted fractures occurred most frequently at the middle of the upper surface of the vertebral body and did not result in wedge-type fractures (Figure 8). Keller *et al*[18] reported that the anterior area of the vertebral body is both less dense and less strong than the posterior region. FE models that take accurate bone density distribution into consideration should thus be created to evaluate fracture risk under such conditions. In addition, to be clinically useful, simulation models should be based on loading conditions that can simulate common activities of daily living. So, based on the fact that strength under forward bending was significantly lower than under uniaxial compression, prediction of strength under forward bending should also be added for further assessment. In any case, assessment of fracture risk using a patient-specific CT-based FE method could contribute to preventing wedge-shaped vertebral fracture by allowing instruction of patients with predicted high risk to avoid various risky postures during activities of daily living.

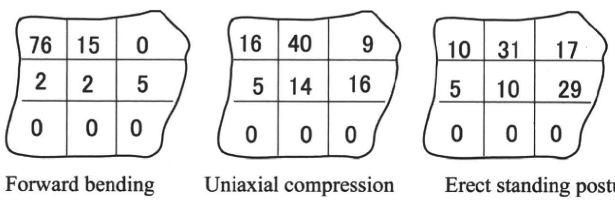

Figure 6. Distributions of predicted fracture sites under each of the loading configurations. Figures were expressed as percentages. Fracture sites tended to be located in the upper third of the vertebral body under all loading configurations. In forward bending, 76% of sites were present in the anterior third.

Vertebral curvature affects the distribution of loading on the endplate of each vertebra. Unfortunately, investigations of load distribution on the end plate *in vivo* have yet to be published. With a mechanical testing machine, Adams *et al*[19] measured load distribution on the end plate of vertebral bodies *in vitro* using a functional spinal unit taken from cadavers. In addition, as the degree of disc degeneration may alter the distribution of load magnitude along the end plate,[18,20,21] distributions of load magnitude on the end plate are quite difficult to determine. Our aim was to provide a quantitative diagnostic tool to accurately evaluate bone fracture risk by taking as many determinant factors for bone strength as possible into consideration. CT-based FEM is the most advanced method to satisfy these demands. Our intention was not to provide a method to decide whether a bone in a certain

Forward bending

zone	1	2	3	4	5	6	7	8	9
1		0	0	0	0	0	0	0	0
2	0		0.00012	ns	ns	ns	0.0003	0.00079	0.00208
3	0	0.00012		ns	ns	ns	ns	ns	ns
4	0	ns	ns		ns	ns	ns	ns	ns
5	0	ns	ns	ns		ns	ns	ns	ns
6	0	ns	ns	ns	ns		ns	ns	ns
7	0	0.0003	ns	ns	ns	ns		ns	ns
8	0	0.00079	ns	ns	ns	ns	ns		ns
9	0	0.00208	ns	ns	ns	ns	ns	ns	

Uniaxial compression

zone	1	2	3	4	5	6	7	8	9
1		ns	ns	ns	ns	ns	ns	ns	ns
2	ns		0.00032	0.00001	0.00354	ns	0	0	0
3	ns	0.00032		ns	ns	ns	ns	ns	ns
4	ns	0.00001	ns		ns	ns	ns	ns	ns
5	ns	0.00354	ns	ns		ns	ns	ns	ns
6	ns	ns	ns	ns	ns		ns	ns	ns
7	ns	0	ns	ns	ns	ns		ns	ns
8	ns	0	ns	ns	ns	ns	ns		ns
9	ns	0	ns	ns	ns	ns	ns	ns	

Erect standing posture

zone	1	2	3	4	5	6	7	8	9
1		ns	ns	ns	ns	ns	ns	ns	ns
2	ns		ns	0.00121	ns	ns	0.00001	0.00002	0.00005
3	ns	ns		ns	ns	0.0015	0.00105	ns	ns
4	ns	0.00121	ns		ns	ns	ns	ns	ns
5	ns	ns	ns	0.0015		ns	ns	ns	ns
6	ns	ns	ns	ns	ns		0	0.00001	0.00004
7	ns	0.00001	0.00105	ns	ns	0		ns	ns
8	ns	0.00002	ns	ns	ns	0.00001	ns		ns
9	ns	0.00005	ns	ns	ns	0.00004	ns	ns	

Zone definition

1	2	3
4	5	6
7	8	9

Figure 7. *P* values calculated using Ryan's method. Each zone was numbered; the antero-superior zone was numbered "1," middle-superior "2," and postero-superior "3." Middle row was numbered from the anterior column "4," "5," "6," and "9" for the postero-inferior zone.

patient would break under a certain mechanical environment. Instead, our approach involved the virtual extraction of a bone of interest from a patient and then examining that bone under virtual static mechanical testing. Predicted strength from this simulation may be far from accurate compared with that derived from more realistic simulations incorporating dynamic analyses or more realistic mechanics. Despite these limitations, CT-based FEM offers a far more advanced method to diagnose bone fragility than the prevailing clinically available bone densitometry. In the future, we intend to adopt more advanced simulation methods, including more realistic loading conditions that reflect the effects of spinal curvature and discs.

Another limitation was that our FE model did not include posterior elements. Previous studies that evaluated vertebral strength using a CT/FE model also excluded posterior elements.[22–24] This does not reflect actual loading configurations in activities of daily living. If the FE model could include posterior elements, simulation of the vertebral body under various loading conditions would be more realistic.

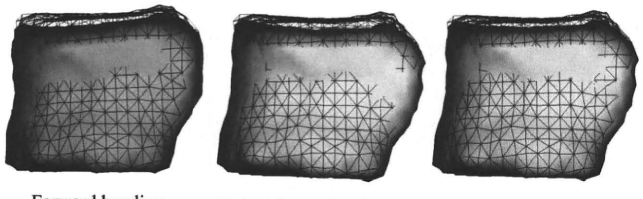

Figure 8. Typical deformation of vertebral body under the 3 loading conditions magnified 10-fold. The anterior part collapsed under forward bending, resulting in wedge-shaped fracture. In uniaxial compression and erect standing, the middle upper part collapsed.

Analyses of fracture risks of vertebrae under loading condition simulating forward bending were performed by Bouxsein *et al*[25] by calculating "factor-of-risk" based on data on loads applied to vertebral bodies investigated by Schultz and Andersson.[26] However, Bouxsein *et al*[25] did not analyze predicted fracture sites.

Crawford[23] investigated rigidity and strain distributions of vertebrae using a linear FE method by inducing bending moment. The correlation between effective bending and axial rigidity of all vertebrae was reportedly R = 0.83. They concluded that axial properties were not necessarily strongly correlated with bending properties. In our study, although a different FE method was adopted from that of Crawford *et al*, the results were not contradictory between these studies. To the best of our knowledge, the present study is the only one to have investigated fracture strength of vertebrae under loading conditions simulating forward bending using a nonlinear FE method. Based on the present results, evaluation of fracture strength in patients with osteoporosis should be evaluated not only with uniaxial compression, but also using a forward-bending loading condition. At present, deriving a simple equation to help make a decision re-